

K.P. Singh
President and CEO
Holtec International

A.I. Soler
Executive Vice President
Holtec International

A Design Procedure for Evaluating the Tube Axial Load due to Thermal Effects in Multi-Pass Fixed Tubesheet Exchangers

The unequal length change of the tubes in various tube passes of a multi-tube pass fixed or floating head tubular exchanger produces axial tube loads which may be substantial in some operating units. This paper provides a rational analysis method, heretofore unavailable to the design community, to quantify the effect of multi-pass thermal expansion on the tube axial load. A numerical example is used to illustrate the solution procedure.

1 Introduction

Shell-and-tube heat exchangers are often designed and fabricated in multiple tube passes. The number of tube passes is defined as the number of times the tubeside fluid transverses the length of the heat exchanger [1, Chap. 1]. In most applications, the temperature of the tubeside fluid changes along the tube length as it exchanges heat with the shellside medium. As a consequence the metal temperature of the tubes varies along the tube length, and also from pass to pass. Therefore, the change in the length of the tubes (due to thermal effects) in different tube passes is unequal. The uneven length change of the tubes rarely poses an operational limitation in U-tube designs where the flexibility of the U-bends helps mitigate the tube axial load. The scenario in a fixed tubesheet exchanger is, however, quite different. The consequence of the difference in the length change of the tubes and the shell is the so-called differential thermal expansion load which is quite often the dominant load on the tubesheet. Industry design standards such as the TEMA standards [2], recognize the significance of the differential thermal expansion load, and include it in the thickness calculation of tubesheets for fixed tubesheet heat exchangers. Strictly speaking, TEMA design rules are only applicable to single tube pass fixed tubesheet exchangers. The only thermal expansion quantity required to be input in the design formulas is the differential thermal expansion between the tube bundle and the shell. The TEMA standards advise the designer to give special consideration to multi-pass designs with "extreme interpass temperature differentials" [2, p. 126]. An unofficial survey of users by the TEMA Technical Committee indicated wide variations in procedures used to calculate the "effective differential thermal expansion" between the tubes and the shell in multi-tube pass designs. Even the recently published book on the mechanical design of heat exchangers [1] which contains several computer codes for

tubesheet stress analysis [3] provides little help in incorporating the effect of unequal temperature changes in different tube passes in a multiple tube pass unit.

To be sure, one can bound the tubesheet design problem by taking the largest shell-to-tube differential expansion occurring in the heat exchanger (usually the first tube pass) as the value for use in the tubesheet design. But this practice leads to excessive conservatism in design and is therefore adopted by few designers and analysts. It is far more common to use an average of the tube bundle metal temperatures for establishing the differential expansion. While this latter practice is perhaps adequate for sizing the tubesheet thickness, it may be unconservative in evaluating the maximum tube axial load. Since the magnitude of the tube axial load directly affects the tube-to-tubesheet joint integrity, it is important to evaluate the maximum tube axial load to within a reliable level of accuracy. This paper provides a practical approach to tackle this problem.

While the preceding introduction focuses on fixed tubesheet constructions, the technique presented in this paper is equally pertinent to floating head designs. The paper is arranged to provide the conceptual framework of the analysis in Section 2 followed by the details in Section 3. A reader unwilling to delve into the process of derivation of the governing equations may proceed directly to Section 4, wherein a step-by-step procedure to carry out a design task is outlined. Section 5, which contains a numerical example, serves to illustrate the calculational procedure.

2 Mathematical Model

In this analysis, the heat exchanger shell is assumed to be subject to a rotationally symmetric temperature change. The axial length change of the tubes due to temperature effects is assumed to be equal in each tube pass, but may be different in different passes. Analytical methods and computer programs presented in reference [1] treat the elastostatic problem of interaction between axial strains in the shell and the tubes, and

Contributed by the Pressure Vessels and Piping Division for publication in the JOURNAL OF PRESSURE VESSEL TECHNOLOGY. Manuscript received by the Pressure Vessels and Piping Division, January 10, 1985; revised manuscript received February 3, 1986.

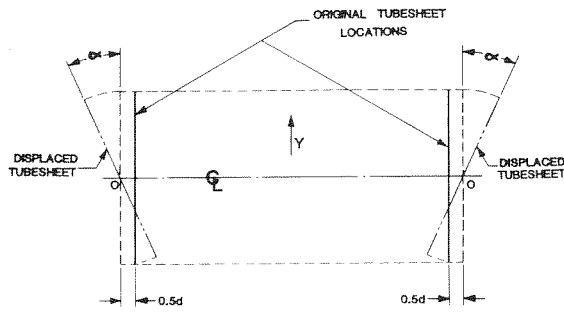


Fig. 1 Tubesheet displacement and rotation

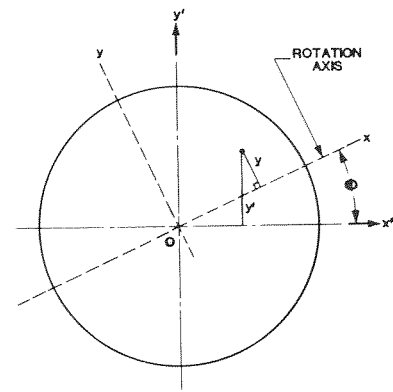


Fig. 2 Coordinate axis transformation

lateral deflection of the tubesheets within the framework of thin plate and shell theories. Our object herein is to express the temperature-induced length change of the aggregate of the tubes as consisting of an axial translation of the tubesheet plus a rotation. The axial movement component is then to be used in the tubesheet design standards [2], and design/stress analysis codes [3]; and the spatially varying rotation component provides the means to assess the magnitude of the added tube axial load. It is heuristically apparent that any lateral compliance of the tubesheet helps reduce the thermal component of the axial load in the tube. Therefore, assuming the tubesheets to be rigid (infinite flexural rigidity) has the effect of making the tube axial load computation conservative. This assumption also has the added advantage of greatly simplifying the analysis—an important consideration in an analysis aimed to help carry out routine design work. It is also noted that, without any loss of generality, we can talk of the length change of tubes with respect to the shell, rather than their absolute length change. Therefore, in what follows, the quantity Δ_i will represent the differential thermal expansion of the tubes in pass i , with respect to the shell.

The mathematical model constructed in this manner leads to the tubesheets undergoing some axial separation and rotation. The participation of the shell in influencing the axial separation of the tubesheet is considered in the subsequent stress analysis of the tubesheet as described in references [1, 4-6, 7-10], or implied in the design formulas of reference [2]. Therefore, in our analysis here, we need not consider the effect of the shell in determining the effective axial separation of the two tubesheets. However, the participation of the shell in modifying the relative rotation of the two tubesheets must be considered here. What this means is that a force equilibrium condition need not include the shell effect, but any moment equilibrium condition will include the effect.

3 Analysis

Using the rigid tubesheet assumption, and considering that the shell extends and bends like a beam, the separation of two points on the two tubesheets at a distance y from the axis of rotation can be expressed as $d + 2\alpha y$; where d is the axial separation and α is the rotation of each tubesheet (Fig. 1). In Fig. 2, we define a coordinate axis set (x', y') in the plane of the tubesheet which may be taken as the natural axes of symmetry of the tube layout pattern. Tubesheet rotation, however, will occur about an axis whose orientation is not yet known. We indicate the axis of tubesheet rotation by coordinate axis x . The axis orthogonal to x will be heretofore denoted as y -axis. The angle ϕ in Fig. 2 denotes the to-be-determined orientation of the rotation axis with respect to the chosen natural axis $(x'$ and y' axes).

If Δ_i and δ_i , respectively, represent the longitudinal thermal expansion of the tube in pass i (over the shell); and elastic stretch of the tube located at distance y from the axis of rotation in pass i (Fig. 2), then displacement continuity requires

$$\Delta_i + \delta_i = d + 2\alpha y \quad (1)$$

According to our assumptions, δ_i is a function of y . The longitudinal strain in a tube of length l corresponding to extension δ_i is δ_i/l . If a_m and A_i represent the metal cross-sectional area of one tube, and the surface area ascribable to pass i on the tubesheet surface, then the stress $E_i\delta_i/l$ in the tube corresponds to the "smeared" surface pressure p_i , on the tubesheet, given by

$$p_i = \frac{n_i a_m}{A_i} \frac{E_i \delta_i}{l} \quad (2)$$

Nomenclature

a_m = metal cross-sectional area of one tube	I_t = planar moment of inertia of tube about its diametral axis	N_t = total number of tubes
A_i = total tubesheet surface area in pass i	J_x = first area moment about axis of rotation	n_i = number of tubes in i th pass
A_{TOT} = total tubesheet area in perforated region	k = axial stiffness of shell per unit circumferential arc length (in units of force/length ²)	p = generic term for "smeared" out pressure due to tube axial load
d = effective longitudinal thermal expansion of tube bundle	l = tube effective length (distance between tubesheet inside faces)	α = effective rotation of each tubesheet
E_s = Young's modulus of shell material at its mean metal temperature	N_p = total number of tube passes	Δ_i = longitudinal thermal expansion of tubes in pass i over shell longitudinal expansion
E_t = Young's modulus of tube material		δ_i = elastic elongation of tubes in i th pass
F_{ax} = axial load in one tube located at coordinate (x', y')		

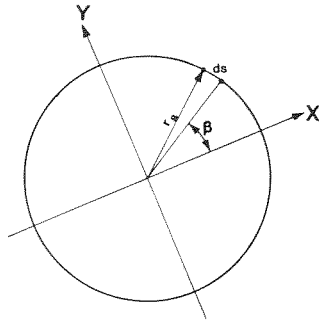


Fig. 3 Shell cross section

where n_i is the number of tubes in pass i .

Substituting for σ_i from equation (1), we have

$$p_i = \frac{E_t a_m n_i}{l A_i} [d + 2\alpha y - \Delta_i] \quad (3)$$

We will now derive equilibrium equations necessary to solve for ϕ , d and α . We recall that ϕ is the angle made by the x -axis with the global coordinate axes, d is the axial separation of point 0 on the two tubesheets, and α is the rotation of each tubesheet.

3 Force Equilibrium

The summation of the surface pressure p over the tubesheet must vanish identically. Hence

$$\int p dA = 0$$

or, in terms of a sum over the number of passes,

$$\sum_{i=1}^{N_p} \int p_i dA_i = 0$$

or

$$\sum_{i=1}^{N_p} \int \frac{E_t a_m n_i}{l A_i} (d + 2\alpha y - \Delta_i) dA_i = 0 \quad (4)$$

Performing the integrations in equation (4), we have

$$\frac{n_i E_t a_m}{l A_i} \left[A_{TOT} d + 2\alpha \sum_{i=1}^{N_p} J_x^i - \sum_{i=1}^{N_p} \Delta_i A_i \right] = 0 \quad (5)$$

where

$$J_x^i = \int_{A_i} y dA_i \quad (6)$$

Let

$$\sum_{i=1}^{N_p} J_x^i = J_x \quad (7a)$$

$$\sum_{i=1}^{N_p} \Delta_i A_i = Q \quad (7b)$$

Then equation (6) simplifies to

$$d A_{TOT} + 2\alpha J_x - Q = 0 \quad (8)$$

Moment Equilibrium About the Rotation Axis (x-Axis)

$$\int p y dA + M_{tube} + M_{shell} = 0 \quad (9)$$

The moment exerted by each tube due to a relative rotation between its ends, 2α , is

$$\frac{2\alpha E_t I_t}{l}$$

Therefore, the moment from N_t tubes is

$$M_t = \frac{2N_t E_t I_t \alpha}{l}; \quad N_t = \sum_{i=1}^{N_p} n_i \quad (10)$$

Equation (10) is written on the premise that the clearance between the tube support plate holes and the tubes precludes a lateral restraint on the tubes for the support plates. In view of the dimensional uncertainties in actual hardware, this is perhaps the most logical assumption. If, however, the lateral contact of baffles can be ensured, then the foregoing expressions for M_t should be appropriately modified.

Similarly, the moment exerted by the shell is (see Fig. 3)

$$M_{shell} = k \int_0^{2\pi} (d + 2\alpha r_s \sin\beta) r_s \sin\beta ds; \quad ds = r_s d\beta$$

or

$$M_{shell} = 2\pi \alpha k r_s^3 \quad (11)$$

where k is the axial stiffness of the shell per unit circumference. If the shell is equipped with an expansion joint then k is computed using the appropriate computer codes, e.g., the programs FLANFLUE or EXJOINT [1, Chap. 15]. The expression for k for a uniform thickness shell without an expansion joint follows from basic strength-of-materials theory.

$$k = \frac{E_s t_s}{l} \quad (11a)$$

E_s and t_s are Young's modulus of the shell material at the average shell metal temperature and its thickness, respectively.

Note that in obtaining equation (11), we have assumed that the shell cross section rotates like a rigid body; i.e., exhibits a beamlike behavior in response to the rotation α .

Finally, the remaining term in equation (9) becomes

$$\int p y dA = \frac{E_t a_m n_i}{A_i l} \sum_{i=1}^{N_p} \int_{A_i} (d + 2\alpha y - \Delta_i) y dA_i$$

or

$$\int p y dA = \frac{n_i E_t a_m}{A_i l} [d J_x + 2\alpha I_{xx} - J_{xx}] \quad (12)$$

where

$$I_{xx} = \sum_{i=1}^{N_p} \int_{A_i} y^2 dA_i = \sum_{i=1}^{N_p} I_{xx}^i \quad (13a)$$

$$J_{xx} = \sum_{i=1}^{N_p} \Delta_i \int_{A_i} y dA_i = \sum_{i=1}^{N_p} \Delta_i J_x^i \quad (13b)$$

From equations (9)-(11), we have

$$\frac{n_i E_t a_m}{l A_i} [d J_x + 2\alpha I_{xx} - J_{xx}] + \frac{2N_t E_t I_t \alpha}{l} + 2\pi \alpha k r_s^3 = 0 \quad (14)$$

Moment Equilibrium About the y-Axis

$$\sum_{i=1}^{N_p} \int_{A_i} p x dA_i = 0$$

or

$$\frac{E_t a_m n_i}{l A_i} \int_{A_i} (d + 2\alpha y - \Delta_i) x dA_i = 0 \quad (15)$$

or

$$d J_y + 2\alpha I_{xy} - J_{yy} = 0 \quad (16)$$

where

$$J_y = \sum_{i=1}^{N_p} \int_{A_i} x dA_i = \sum_{i=1}^{N_p} J_y^i \quad (17a)$$

$$I_{xy} = \sum_{i=1}^{N_p} \int_{A_i} xy dA_i = \sum_{i=1}^{N_p} I_{xy}^i \quad (17b)$$

$$J_{yy} = \sum_{i=1}^{N_p} \Delta_i \int_{A_i} x dA_i = \sum_{i=1}^{N_p} \Delta_i J_y^i \quad (17c)$$

We now need to express the integrals in equations (7), (13), and (17) in terms of the coordinates referenced to in our chosen coordinate system (primed coordinates in Fig. 2). We note that

$$x = x' \cos \phi + y' \sin \phi \quad (18a)$$

$$y = y' \cos \phi - x' \sin \phi \quad (18b)$$

Therefore

$$J_x^i = [y dA_i] = [(y' \cos \phi - x' \sin \phi) dA_i]$$

or

$$J_x^i = J_x'^i \cos \phi - J_y'^i \sin \phi \quad (19)$$

where $J_x'^i$ and $J_y'^i$ are defined in the same manner as J_x^i and J_y^i , respectively, defined earlier. Hence

$$J_x = J_x' \cos \phi - J_y' \sin \phi \quad (20)$$

where

$$J_x' = \sum_{i=1}^{N_p} J_x'^i; \quad J_y' = \sum_{i=1}^{N_p} J_y'^i; \quad \text{etc.}$$

$$I_{xx}^i = [y^2 dA_i] \\ = [(y' \cos \phi - x' \sin \phi)^2 dA_i]$$

or

$$I_{xx}^i = \cos^2 \phi I_{x'x'}^i + \sin^2 \phi I_{y'y'}^i - 2I_{x'y'}^i \sin \phi \cos \phi \quad (21)$$

$$J_{xx} = \sum_{i=1}^{N_p} \Delta_i J_x = \sum_{i=1}^{N_p} J_x'^i \Delta_i \cos \phi - \sum_{i=1}^{N_p} J_y'^i \Delta_i \sin \phi$$

or

$$J_{xx} = J_{x'x'} \cos \phi - J_{y'y'} \sin \phi \quad (22)$$

Referring to equation (17)

$$J_y = \sum_{i=1}^{N_p} \int_{A_i} x dA_i \\ = \sum_{i=1}^{N_p} \int_{A_i} (x' \cos \phi + y' \sin \phi) dA_i$$

or

$$J_y = J_{y'y'} \cos \phi + J_{x'x'} \sin \phi \quad (23)$$

$$I_{xy} = \sum_{i=1}^{N_p} \int_{A_i} xy dA_i \\ = \sum_{i=1}^{N_p} \int_{A_i} (x' \cos \phi + y' \sin \phi)(y' \cos \phi - x' \sin \phi) dA_i$$

or

$$I_{xy} = \cos^2 \phi I_{x'y'}^i - I_{y'y'}^i \sin \phi \cos \phi + I_{x'x'}^i \sin \phi \cos \phi \quad (24)$$

where

$$I_{x'x'}^i = \sum_{i=1}^{N_p} \int_{A_i} y'^2 dA_i; \quad \text{etc.}$$

Finally,

$$J_{yy} = \sum_{i=1}^{N_p} \Delta_i [x dA_i] \\ = \sum_{i=1}^{N_p} \Delta_i \int_{A_i} (x' \cos \phi + y' \sin \phi) dA_i$$

or

$$J_{yy} = J_{y'y'} \cos \phi + J_{x'x'} \sin \phi \quad (25)$$

Using the foregoing relationships, the foregoing three equilibrium equations can be rewritten in terms of integrals involving the primed coordinates.

The force equilibrium equation (equation (8)) becomes

$$[dA_{TOT} + 2\alpha(J_{x'} \cos \phi - J_{y'} \sin \phi) - Q] = 0 \quad (26)$$

Moment equilibrium about x -axis (equation (14)) takes the form

$$\frac{E_t a_m n_i}{l A_i} [d(J_{x'} \cos \phi - J_{y'} \sin \phi) + 2\alpha(\cos^2 \phi I_{x'x'}^i \\ + \sin^2 \phi I_{y'y'}^i - 2\sin \phi \cos \phi I_{x'y'}^i) - J_{x'x'} \cos \phi \\ + J_{y'y'} \sin \phi] + \frac{2N_t E_t I_t \alpha}{l} + 2\pi \alpha k r_s^3 = 0 \quad (27)$$

The third equilibrium equation (equation (16)) becomes

$$d[J_{y'} \cos \phi + J_{x'} \sin \phi] + 2\alpha[\cos^2 \phi I_{x'y'}^i \\ - \sin \phi \cos \phi I_{y'y'}^i + \sin \phi \cos \phi I_{x'x'}^i] \\ - J_{y'y'} \cos \phi - J_{x'x'} \sin \phi = 0 \quad (28)$$

The three simultaneous equations (26)–(28) furnish the necessary relationships to solve for ϕ , α , and d . Any standard nonlinear equation solver routine can be used to solve the problem.

Having determined d , α , and ϕ , the pressure p_i in pass i follows from equations (3) and (18)

$$p_i = \frac{n_i E_t a_m}{l A_i} [d - \Delta_i + 2\alpha(y' \cos \phi - x' \sin \phi)] \quad (29)$$

Therefore, the tube axial load in pass i , due to the multi-pass effect, is

$$F_{ax} = \frac{E_t a_m}{l} [d - \Delta_i + 2\alpha(y' \cos \phi - x' \sin \phi)] \quad (30)$$

where the particular values used for x' , y' , are those appropriate to pass i . This load is in addition to the axial tube load produced by the elastic interaction of the shell, tubes and the tubesheet when all of the Δ_i are the same. As stated before, methods to evaluate the latter are widely available [1, Chap. 9]. A nonzero value for F_{ax} arises only if at least one of the Δ_i are different from the other values of Δ_i .

4 Solution Procedure

It is assumed that the incremental thermal expansion of the tubes over the shell in each tube pass is known from the thermal design of the heat exchanger. In addition to Δ_i , the following additional quantities must be known to conduct the analysis: the number of passes, N_p ; number of tubes in each pass n_i , tube wall thickness, tube outer radius, tube length l , layout pitch and layout angle, and Young's modulus of the tube material. The tube layout grid on the tubesheet surface is assumed to be known, such that the geometric dimensions of each pass can be defined.

Finally, the axial stiffness of the shell k is assumed to be known. Equation (11a) gives k for a shell without an expansion joint. For a fixed tubesheet exchanger equipped with an expansion joint, k is primarily dictated by the axial com-

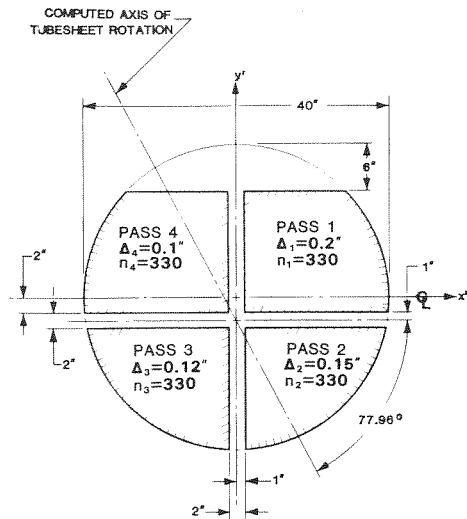


Fig. 4 Tube layout for the example problem

pliance of the expansion joint [1, Chap. 15]. k is zero for a floating head unit.

The solution procedure proceeds in the following three steps:

(i) Evaluate elementary data: The tube metal area a_m follows directly from the tube outer radius and tube wall. The area on the tubesheet surface imputable to one tube is known from the layout pitch and layout angle.

(ii) Area integrals: Select a set of natural axes (primed axes in Fig. 2). Evaluate the integrals J_x^i (equation (6)), I_{xx}^i and J_x^i (equation (13)), J_y^i , I_{xy}^i and J_y^i (equation (17)) for each pass ($i = 1, 2, \dots, N_p$). From the summations J_x , Q (equation (7)), I_{xx} , J_{xx} (equation (13)), and J_y , I_{xy} (equation (17)) can be determined.

(iii) Solve the three simultaneous equations (equations (26)–(28)) in the three unknowns d , α and ϕ . Use equation (30) to compute the axial tube load F_{ax} in a tube located at coordinate (x', y') .

Computer program MUTEX [3] performs the foregoing analysis, as illustrated in the next section.

5 An Example

Let us consider a four-pass fixed tubesheet exchanger, containing 330 tubes, 3/4 in. diameter \times 18 BWG (0.049 in. nominal wall) in each pass. The tubes are laid out on 0.9375 in. pitch in 4-pass arrangement as shown in Fig. 4. All tubes are contained in a 20-in. radius circle; the shell inside radius r_s is 20.75 in. The relative thermal expansion of the tubes over the shell is given as:

- Tubes in pass 1, $\Delta_1 = 0.20$ in.
- Tubes in pass 2, $\Delta_2 = 0.15$ in.
- Tubes in pass 3, $\Delta_3 = 0.12$ in.
- Tubes in pass 4, $\Delta_4 = 0.10$ in.

Other data required to define the problem are:

- Tube length between the tubesheets: 15 ft = 180 in.
- Tube material Young's Modulus, $E_t = 25 \times 10^6$ psi
- Shell material Young's Modulus, $E_s = 30 \times 10^6$ psi
- Shell wall thickness, $t_s = 0.375$ in.

In the absence of an expansion joint, the shell axial stiffness is given by equation (11a).

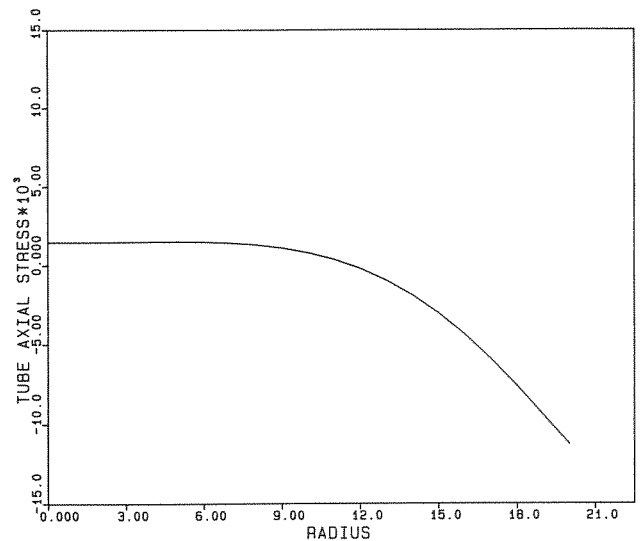


Fig. 5 Tube axial stress distribution due to uniform linear differential expansion, d

$$k = \frac{(30 \times 10^6)(0.375)}{(180)} = 62500 \text{ psi}$$

The area integrals for this data set, computed by program MUTEX, are as follows:

$$\begin{aligned} J_x' &= 1927; & J_y' &= 0, & I_{xx}' &= 96648 \\ J_{yy}' &= 127079, & I_{xy}' &= 0, & J_{xx}' &= -211 \\ J_{yy}' &= 361, & Q &= 152 \end{aligned}$$

Solving equations (26)–(28) using the computer code MUTEX yields the following answer:

$$\begin{aligned} d &= 0.1438 \text{ in.} \\ \alpha &= 0.834 \times 10^{-3} \text{ rad} \\ \phi &= -1.36 \text{ rad} = -77.96 \text{ deg} \end{aligned}$$

The tube loading at a point y from the rotation axis due to the multi-pass effect is given by equation (30).

$$F_{ax} = \frac{E_t a_m}{l} [0.1438 - \Delta_i + 2\alpha y]$$

where the tube metal area a_m is given by

$$a_m = \pi(0.75 - 0.049)(0.049) = 0.1079 \text{ in}^2$$

Hence, the tube axial load in pass 1 is

$$F_{ax} = 14986(0.143 - 0.2 + 1.668 \times 10^{-3}y)$$

or

$$F_{ax} = 149.86(-5.62 + 0.167y)$$

Therefore, the tube load in pass 1 varies from a minimum value of -820 lb in the tube nearest to the rotational axis (shown by dotted line in Fig. 4) to a maximum value of -341 lb at the outer bundle periphery, $y = 20$ in. This corresponds to a tube compressive stress of over 7600 psi in the inner tube and 3166 psi at the periphery tube.

In the second step of the analysis, the tube load and tubesheet stress due to the average differential expansion d is required. For this purpose, computer program FIXSHEET [3, Part B], was used. FIXSHEET performs an elastostatic interaction analysis of the shell, channel, tubesheet, and tubes. For this illustration, the tubesheet and channel thicknesses were specified as 2 in. and 0.375 in., respectively. Both end channels are assumed to be integrally welded to the two tubesheets, respectively. The equivalent Young's modulus and Poisson's ratio of the perforated tubesheet material is estimated from Fig. 8.1.1 of reference [1] to be 8.4×10^6 psi

and 0.35, respectively. The channel material properties are assumed to be identical to those of the shell. The maximum tube axial stress is plotted as a function of the radius (from the axis of symmetry) in Fig. 5. The maximum tube compressive stress is found to develop at the outer periphery tubes and is equal to 11,270 psi. It is noted that the additional tube compressive stress due to the multi-pass effect of 3166 psi at this location is over 28 percent of the axisymmetric analysis value. It obviously should not be ignored where operational reliability of the tube-to-tubesheet joint is important.

6 Closure

A practical design technique has been devised to determine the added tube axial load due to unequal tube expansion in the various passes of a multiple tube pass fixed or floating head exchangers. Inspection of an illustrative example shows that the added tube load multiple pass effect can be substantial in commonplace situations, and therefore should not be ignored, as has been the practice in the industry until now.

It is believed that inclusion of this load would foster a better understanding of the failure sequence of tubes in operating units. Furthermore, it should provide the analyst/designer the necessary tools to avoid multi-pass tube designs with perilously high tube loads.

The axial tube load, in addition to affecting the tube joint life, has a pronounced influence on the likelihood of destructive flow induced vibration of the tube. High compressive tube loads depress the tube fundamental natural frequency which can increase the potential of a flow induced vibration failure

[1, Chap. 16]. The method presented herein should help identify such a problem at the design stage.

Acknowledgment

The authors are thankful to Mr. Teik-Lee Ng for his help in the programming and debugging of the code MUTEX.

References

- 1 Singh, K. P., and Soler, A. I., *Mechanical Design of Heat Exchangers and Pressure Vessel Components*, Arcturus Publishers, Inc., Cherry Hill, N.J., 1984.
- 2 *Standards of Tubular Exchanger Manufacturers Association*, Sixth Edition, TEMA, Inc., Tarrytown, N.Y., 1978.
- 3 Singh, K. P., Soler, A. I., and Ng, Teik-Lee, *HEXDES User Manual*, Arcturus Publishers, Inc., Cherry Hill, N.J., 1984.
- 4 Gardner, K. A., "Heat Exchanger Tubesheet Design - 2 Fixed Tubesheets," *ASME Journal of Applied Mechanics*, Vol. 74, 1952, pp. 159-166.
- 5 Miller, K. A. G., "The Design of Tube Plates of Heat Exchangers," *Proceedings of the Institution of Mechanical Engineers*, Ser. B, Vol. 1, 1951, pp. 215-231.
- 6 Boon, G. B., and Walsh, R. A., "Fixed Tubesheet Heat Exchangers," *ASME Journal of Applied Mechanics*, Vol. 86, 1964, pp. 175-180.
- 7 Singh, K. P., "Analysis of Vertically Mounted Through-tube Heat Exchangers," *ASME Journal of Engineering for Power*, Vol. 100, 1978, pp. 380-390.
- 8 Singh, K. P., and Soler, A. I., "A Design Concept for Maximizing Stress Levels in Stationary Tubesheet Heat Exchangers," *International Journal of Pressure Vessels and Piping*, Vol. 13, 1983, pp. 19-32.
- 9 Chiang, C. C., "Structural Design Optimization of Once-through Type Heat Exchangers," ASME Paper No. 77-JPGC-NE-3, 1977.
- 10 Hayashi, K., "An Analysis Procedure for Fixed Tubesheet Heat Exchangers," *Proceedings of the Third International Conference on Pressure Vessel Technology: Part I, Analysis, Design and Inspection*, ASME, New York, 1977, pp. 363-373.